

Leaving Group Assistance in the La³⁺-Catalyzed Cleavage of Dimethyl (*o*-Methoxycarbonyl)aryl Phosphate Triesters in Methanol

David R. Edwards, C. Tony Liu, Graham E. Garrett, Alexei A. Neverov, and R. Stan Brown*

Department of Chemistry, Queen's University, Kingston, Ontario, Canada K7L 3N6

Received June 18, 2009; E-mail: rsbrown@chem.queensu.ca

Abstract: The catalytic methanolysis of a series of dimethyl aryl phosphate triesters where the aryl groups contain an *o*-methoxycarbonyl (*o*-CO₂Me) substituent (**4a–i**) was studied at 25 °C in methanol containing La³⁺ at various concentrations and pH . Determination of the second-order rate constant for La³⁺-catalyzed cleavage of substrate **4a** (dimethyl (*o*-methoxycarbonyl)phenyl phosphate) as a function of pH was assessed in terms of a speciation diagram that showed that the process was catalyzed by La³⁺(⁻OCH₃)_{*x*} dimers, where *x* = 1–5, that exhibit only a 5-fold difference in activity between all the species. The second-order catalytic rate constants (*k*₂^a) for the catalyzed methanolysis of **4a–i** at pH 8.7 fit a Brønsted relationship of $\log k_2^a = (-0.82 \pm 0.11)\text{p}K_{\text{a}}^{\text{H}} + (11.61 \pm 1.48)$, where the gradient is shallower than that determined for a series of dimethyl aryl phosphates that do not contain the *o*-CO₂Me substituent, $\log k_2^a = (-1.25 \pm 0.06)\text{p}K_{\text{a}}^{\text{H}} + (16.23 \pm 0.75)$. Two main observations are that (1) the *o*-CO₂Me group preferentially accelerates the cleavage of the phosphate triesters with poor leaving groups relative to those with good leaving groups and (2) it provides an increase in cleavage rate relative to those of comparable substrates that do not have that functional group, e.g., $k_2^a(\text{dimethyl } o\text{-methoxycarbonylphenyl phosphate})/k_2^a(\text{dimethyl phenyl phosphate}) = 60$. Activation parameters for the La³⁺-catalyzed methanolysis of **4a** and dimethyl 4-nitrophenyl phosphate show respective ΔH^\ddagger (ΔS^\ddagger) values of 3.3 kcal/mol (–47 cal/mol·K) and 0.7 kcal/mol (–46.5 cal/mol·K). The data are analyzed in terms of a concerted reaction where the catalytic complex (La³⁺(⁻OCH₃)_{*x-1*}) binds to the three components of a rather loose transition state composed of a nucleophile CH₃O⁻, a nucleofuge ⁻OAr, and a central (RO)₂P²⁺–O⁻ in a way that provides leaving group assistance to the departing aryloxy group.

1. Introduction

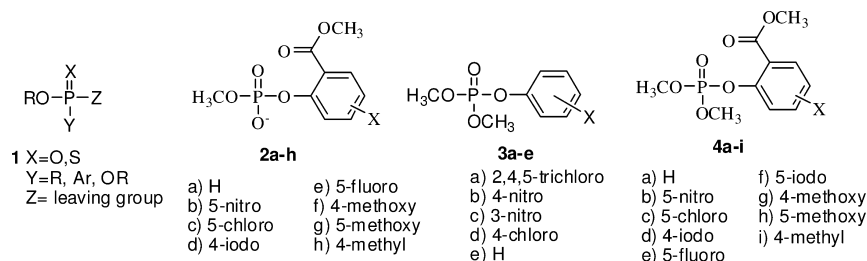
Phosphate triesters are not naturally occurring molecules and so have no known natural biological function. However man-made organophosphate (OP) pesticides and chemical weapons (CW) of general structure **1** (Chart 1), where LG is a leaving group with $\text{p}K_{\text{a}} \leq 8$, are strong acetylcholinesterase inhibitors.¹ The OP pesticides have important uses as animal and crop protectants² but are under increasing regulatory scrutiny due to toxicity and environmental persistence. Phosphotriesterase (PTE) enzymes produced by soil-dwelling bacteria, while having no known naturally occurring substrates, are very effective at destroying neutral OP pesticides, thereby protecting the organism from poisoning. The two most studied PTEs, from *Agrobacterium radiobacter* and *Pseudomonas diminuta*, are dinuclear Zn(II) enzymes that have nearly 90% amino acid homology and

conserve all the metal-binding ligands.³ While not exactly established, the mechanism of action of these has been discussed as involving intramolecular delivery of a Zn(II)-coordinated hydroxide (possibly one bridged between the two Zn(II) ions) to a phosphate ester substrate which is transiently activated by P=O coordination to the second Zn(II) ion.⁴ This sort of dinuclear core is characteristic of other enzymes that mediate hydrolytic cleavage of phosphate diesters⁵ and monoesters⁶ and gives the *P. diminuta* bacterium the ability to hydrolyze paraoxon, its preferred substrate, with an efficiency near the diffusion limit, $k_{\text{cat}}/K_{\text{M}} \approx 10^8 \text{ M}^{-1} \text{ s}^{-1}$.⁷

- (1) (a) Main, R. A.; Iverson, F. *Biochem. J.* **1966**, *100*, 525. (b) Emsley, J.; Hall, D. *The Chemistry of Phosphorus*; Wiley: New York, 1976; p 494.
 (2) (a) Toy, A.; Walsh, E. N. *Phosphorus Chemistry in Everyday Living*, 2nd ed.; American Chemical Society: Washington, DC, 1987; Chapters 18–20. (b) Quin, L. D. *A Guide to Organophosphorus Chemistry*; Wiley: New York, 2000. (c) Gallo, M. A.; Lawryk, N. J. *Organic Phosphorus Pesticides. The Handbook of Pesticide Toxicology*; Academic Press: San Diego, CA, 1991.

- (3) Yang, H.; Carr, P. D.; McLoughlin, S. Y.; Liu, J. W.; Horne, I.; Qiu, X.; Jeffries, C. M. J.; Russell, R. J.; Oakeshott, J. G.; Ollis, D. L. *Protein Eng.* **2003**, *16*, 135.
 (4) (a) Jackson, C. J.; Foo, J.-L.; Kim, H.-K.; Carr, P. D.; Liu, J.-W.; Salem, G.; Ollis, D. L. *J. Mol. Biol.* **2008**, *375*, 1189, and references therein. (b) Kim, J.; Tsai, P.-C.; Chen, S.-L.; Himo, F.; Almo, S. C.; Rauschel, F. M. *Biochemistry* **2008**, *47*, 9497, and references therein.
 (5) (a) Lipscomb, W.; Sträter, N. *Chem. Rev.* **1996**, *96*, 2375. (b) Collman, J. E. *Curr. Opin. Chem. Biol.* **1998**, *2*, 222. (c) Cowan, J. A. *Chem. Rev.* **1998**, *98*, 1067. (d) Davies, J. F.; Hostomska, Z.; Hostomsky, Z.; Jordan, S. R.; Mathews, D. A. *Science* **1991**, *252*, 88. (e) Beese, L. S.; Steitz, T. A. *EMBO J.* **1991**, *10*, 25. (f) Lahm, A.; Volbeda, S.; Suck, D. *J. Mol. Biol.* **1990**, *215*, 207.
 (6) Gani, D.; Wilke, J. *Chem. Soc. Rev.* **1995**, *24*, 55.
 (7) Omburo, G. A.; Kuo, J. M.; Mullens, L. S.; Rauschel, F. M. *J. Biol. Chem.* **1992**, *267*, 13278.

Chart 1



There are several man-made metal-ion-containing catalysts that promote the hydrolysis and alcoholysis of phosphate triesters and related neutral OP esters.^{8–10} Studies of these systems have helped define the modes by which metal ions can facilitate the cleavage of neutral OP esters as well as phosphate esters in general:^{8a} (1) via Lewis acid activation of the phosphate ester by metal ion coordination to the phosphoryl oxygen; (2) by nucleophile activation via solvent coordination to the metal ion to reduce its pK_a and generate an active M⁺–[–]OR species; and (3) by providing leaving group assistance (LGA) via coordination of the departing oxyanion to a metal ion, thereby facilitating P–OLG bond cleavage (OLG = leaving group). Recently we reported a simple artificial phosphotriesterase system comprising La³⁺ in methanol that is highly catalytic for the cleavage of neutral phosphates and phosphorothioates,¹⁰ phosphonates,¹¹ and phosphonothioates,¹² the latter two OP materials being taken as models for the G- and V-classes of nerve agents. The Brønsted plot determined for the La³⁺-catalyzed reaction of diethyl aryl phosphates at a nearly neutral pH of 9.1 in methanol^{13,14} fits a linear regression of $\log k_{\text{cat}}^{\text{L}} = (-1.43 \pm 0.05)\text{p}K_{\text{a}}^{\text{HOAr}} - (17.60 \pm 1.07)$. The large gradient of the line (β_{lg}) signifies that the catalyzed process has a very loose transition state (TS)¹⁵ with a high degree of P–OAr bond cleavage, which is very similar to the situation believed to occur

in PTE, where the β_{lg} is reported to be -1.8 to -2.2 .¹⁶ The extent of bond cleavage in the La³⁺-catalyzed reaction is far greater than for the methoxide-catalyzed process, where the β_{lg} was determined to be -0.70 ± 0.05 .^{10c} The results for both the enzymatic and La³⁺ systems were rationalized by invoking the first two proposed modes of metal ion catalysis, namely Lewis acid activation of the bound substrate and intramolecular delivery of a metal-ion-coordinated nucleophile. However, for each system LGA was explicitly rejected as being inconsistent with the large negative β_{lg} values.^{10c,17}

Leaving group assistance by metal ions has been difficult to demonstrate in the cleavage of phosphate diesters¹⁸ and more so for phosphate triesters,¹⁹ although the closely related general acid assistance of the cleavage of di-²⁰ and triesters²¹ has been amply documented. Our recent studies demonstrated LGA by a dinuclear Zn(II):([–]OCH₃) complex during its catalytic cleavage of some specific methyl aryl phosphates having *o*-methoxycarbonyl (*o*-CO₂Me) and nitro groups in essentially neutral methanol.^{22a} Similarly, Yb³⁺ exhibits LGA of the methanolytic cleavage of a series of methyl (*o*-methoxycarbonyl)aryl phosphate diesters (**2a–h**, Chart 1) in acidic methanol.^{22b} The *o*-CO₂Me substituent was suggested to play the key role of transiently coordinating to the metal ion, thereby positioning the Yb³⁺ to provide a 10¹² acceleration for the methanolytic cleavage of the P–OAr bond.^{22b}

The ability of the *o*-CO₂Me group to bring about such large LGA for the Yb³⁺-promoted methanolysis of phosphate diesters spurred this investigation of whether a similar effect would be operative in the La³⁺-catalyzed cleavage of phosphate triesters **3a–e** vs **4a–i** (Chart 1). While one might wonder whether LGA is even remotely required for a process where there is already such significant P–OAr cleavage as in the La³⁺-catalyzed methanolysis of diethyl aryl phosphates, herein we show that the departure of the *o*-CO₂Me-substituted aryloxy group is subject to LGA in the La³⁺-promoted cleavage of **4**. LGA is

- (8) (a) Williams, N. H.; Takasaki, B.; Wall, M.; Chin, J. *Acc. Chem. Res.* **1999**, *32*, 485. (b) Weston, J. *Chem. Rev.* **2005**, *105*, 2152. A compendium of works to 2005 is found in refs 5 and 6 of citation 10c.
- (9) (a) Klinkel, K. L.; Kiemele, L. A.; Gin, D. L.; Hagadorn, J. R. *J. Mol. Catal. A* **2007**, *267*, 173. (b) Aguilar-Perez, F.; Gomez-Tagle, P.; Collado-Fregoso, E.; Yatsimirsky, A. K. *Inorg. Chem.* **2006**, *45*, 9502. (c) Sanchez-Lombardo, I.; Yatsimirsky, A. K. *Inorg. Chem.* **2008**, *47*, 2514. (d) Morrow, J. R.; Trogler, W. C. *Inorg. Chem.* **1988**, *27*, 3387.
- (10) (a) Tsang, J. S.; Neverov, A. A.; Brown, R. S. *J. Am. Chem. Soc.* **2003**, *125*, 7602. (b) Tsang, J. S. W.; Neverov, A. A.; Brown, R. S. *Org. Biomol. Chem.* **2004**, *2*, 3457. (c) Liu, T.; Neverov, A. A.; Tsang, J. S. W.; Brown, R. S. *Org. Biomol. Chem.* **2005**, *3*, 1525.
- (11) Lewis, R. E.; Neverov, A. A.; Brown, R. S. *Org. Biomol. Chem.* **2005**, *3*, 4082.
- (12) Melnychuk, S. A.; Neverov, A. A.; Brown, R. S. *Angew. Chem., Int. Ed.* **2006**, *45*, 1767.
- (13) The nomenclature for pH in methanol is described by Bosch and co-workers¹⁴ as per recommendations of the IUPAC: *Compendium of Analytical Nomenclature. Definitive Rules 1997*, 3rd ed.; Blackwell: Oxford, UK, 1998. pH is used for the measured pH of an aqueous solution when the measuring electrode is calibrated with aqueous buffers; if the electrode is calibrated in water and the “pH” of the neat methanol solution is measured, the term pH is used, and if a correction factor of -2.24 is subtracted from the latter reading, then the term pH is used to designate the “pH” measured in the methanol solution and referenced to the same solvent.
- (14) Since the K_{auto} of methanol is $10^{-16.77}$ M², neutral pH is 8.4: Bosch, E.; Rived, F.; Rosés, M.; Sales, J. *J. Chem. Soc., Perkin Trans. 2* **1999**, 1953.
- (15) Hengge, A. C. *Adv. Phys. Org. Chem.* **2005**, *40*, 49.

- (16) (a) Caldwell, S. R.; Newcomb, J. R.; Schlecht, K. A.; Raushel, F. M. *Biochemistry* **1991**, *30*, 7438. (b) Hong, S.-B.; Raushel, F. M. *Biochemistry* **1996**, *35*, 1094.
- (17) Aubert, S. D.; Li, Y.; Raushel, F. M. *Biochemistry* **2004**, *43*, 5707.
- (18) (a) Browne, K. A.; Bruice, T. C. *J. Am. Chem. Soc.* **1992**, *114*, 4951. (b) Dempcy, R. O.; Bruice, T. C. *J. Am. Chem. Soc.* **1994**, *116*, 4511. (c) Bruice, T. C.; Tsubouchi, A.; Dempcy, R. O.; Olson, L. P. *J. Am. Chem. Soc.* **1996**, *118*, 9867.
- (19) Morrow, J. R.; Trogler, W. C. *Inorg. Chem.* **1989**, *28*, 2330.
- (20) (a) Kirby, A. J.; Lima, M. F.; da Silva, D.; Roussev, C. D.; Nome, F. *J. Am. Chem. Soc.* **2006**, *128*, 16944. (b) Mikkola, S.; Stenman, E.; Nurmi, K.; Youseffi-Salakdeh, E.; Stromberg, R.; Lonnberg, H. *J. Chem. Soc., Perkin Trans. 2* **1999**, 1619. (c) Irisawa, M.; Takeda, N.; Komiyama, M. *J. Chem. Soc., Chem. Commun.* **1995**, 1221. (d) Komiyama, M.; Matsumoto, Y.; Takahashi, H.; Shiiba, T.; Tsuzuki, H.; Yajima, H.; Yashiro, M.; Sumaoka, J. *J. Chem. Soc., Perkin Trans. 2* **1999**, 691.
- (21) (a) Kirby, A. J.; Tondo, D. W.; Medeiros, M.; Souza, B. S.; Priebe, J. S.; Lima, M. F.; Nome, F. *J. Am. Chem. Soc.* **2009**, *131*, 2023. (b) Asaad, N.; Kirby, A. J. *J. Chem. Soc., Perkin Trans. 2* **2002**, 1708.

evidenced by (1) a rate enhancement relative to phosphate esters not having this *ortho*-substituent and (2) a reduction in the Brønsted β value from -1.25 for substrates **3** to -0.82 for substrates **4**. Furthermore, we show that the catalytic TS with **4** has a degree of P–OAr cleavage similar to that observed for the La³⁺-promoted cleavage of phosphates **3** and one that is significantly looser than that for the corresponding methoxide-promoted reaction.

2. Experimental Section

a. Materials. Methanol (99.8% anhydrous), La(CF₃SO₃)₃, tetrabutylammonium methoxide (1.0 M solution in methanol, titrated against N/50 certified standard aqueous HCl solution), HClO₄ (70% aqueous solution, titrated to be 11.40 M), sodium hydride (60% dispersion in mineral oil), phenol (99+%), 4-nitrophenol, 3-nitrophenol (99%), 4-chlorophenol (99+%), 2,4,5-trichlorophenol (98%), methyl salicylate (>99%), methyl 5-chlorosalicylate (97%), methyl 4-iodosalicylate (97%), methyl 5-fluoro-2-benzoate (97%), methyl 5-methoxysalicylate (98%), 2-chloro-4-nitrophenol (97%), 3-methyl-4-nitrophenol (98%), 4-chlorophenol (99+%), 3-methoxyphenol, dimethyl chlorophosphate (96%), diethyl chlorophosphate (97%), methyl 4-methoxysalicylate (98%), methyl 4-methylsalicylate (98%), methyl 2-hydroxy-5-nitrobenzoate (98%), methyl 5-iodosalicylate (99%), and methyl thiosalicylate (97%) were commercial and used as supplied. Phosphate esters **3** and **4** were synthesized according to a general method²³ (see Supporting Information). Each of **3a–e** and **4a–i** had ¹H NMR, ³¹P NMR, and exact MS spectra consistent with the structure (see Supporting Information).

b. Methods. The $\text{p}K_{\text{a}}$ values in methanol for the phenol leaving groups of **3b–d** and **4a–e,g–i** were obtained from previous work.²² The $\text{p}K_{\text{a}}$ of the phenol of **3a** in methanol was determined from the reported relationship $\text{p}K_{\text{a}}^{\text{MeOH}} = (1.08 \pm 0.03)\text{p}K_{\text{a}}^{\text{water}} + (3.50 \pm 0.20)$.^{22a} The $\text{p}K_{\text{a}}$ of the phenol of **4f** was determined by half-neutralization with NaOMe in methanol, and the CH₃OH₂⁺ concentrations were determined potentiometrically using a combination glass electrode (Fisher Scientific Accumet electrode model 13-620-183A) calibrated with certified standard aqueous buffers (pH = 4.00 and 10.00) as described previously. The pH values in methanol were determined by subtracting the correction constant of -2.24 from the electrode readings as described.¹⁰

c. General UV/Visible Kinetics. La³⁺-catalyzed reactions were monitored by UV/vis spectrophotometry under buffered conditions (18.4 mM *N*-*i*Pr-morpholine containing 0.5 equiv of HClO₄) at pH 8.7. Reactions were initiated by the addition of 5×10^{-5} M phosphate ester into standard 1 cm path length UV cuvettes containing the buffered solution of La(OTf)₃ in methanol. Reaction progress was monitored for **4a,c,d,h** at 343 nm, **4b** at 330 nm, **4e,g,i** at 340 nm, **4f** at 370 nm, **3a** at 303 nm, **3b** at 268 nm, **3d** at 286 nm, and **3e** at 290 nm to obtain pseudo-first-order rate constants (k_{obs}) at each [La(OTf)₃]. Since previous work¹⁰ has demonstrated that La³⁺(⁻OCH₃)_x dimers comprise the bulk of the active species at the [La³⁺] concentrations used, the gradients of the k_{obs} versus [La]_{total}/2 plots were used to give the second-order rate constants (k_2^{a}). The pH/rate profile for the La³⁺-catalyzed cleavage of **4a** (4×10^{-5} M) was determined at constant [La]_{total} = 1.1 mM with varying amounts of added NBu₄OCH₃ (0.25–3.1 mM), and the pH of the methanol solutions was measured following complete reaction. The base-catalyzed reactions of substrates **3** and **4a,b,d,e,f,h** were initiated by the addition of 0.02–0.06 M NaOCH₃ to 1 cm UV cuvettes containing 1×10^{-4} M phosphate ester, and the reaction progress was monitored at the λ_{max} for the phenolate

product. Second-order rate constants (k_2^{OMe}) were determined from the slopes of the linear plots of k_{obs} versus [NaOCH₃].

d. Activation Parameters for the ⁻OCH₃-Catalyzed and La³⁺-Catalyzed Methanolysis of **4a.** The temperature dependence of k_2^{a} was investigated by determining the k_{obs} values in duplicate for the methanolysis of **4a** at six temperatures from 11 to 52 °C using 1.5 mM La(OTf)₃, pH 8.7. The k_2^{La} constants were determined by dividing the k_{obs} values by [La]_{total}/2. Fitting of the k_2^{a} vs 1/*T* data to the Eyring equation gave ΔH^\ddagger and ΔS^\ddagger values of 3.3 ± 0.1 kcal/mol and -47.0 ± 0.4 cal/mol·K, respectively. The activation parameters for the methoxide-promoted reaction of **4a** were determined analogously from the k_2^{OMe} values at six temperatures between 12 and 50 °C, giving ΔH^\ddagger and ΔS^\ddagger values of 15.6 ± 0.3 kcal/mol and -17.4 ± 0.95 cal/mol·K, respectively.

e. Identification of Reaction Products of the La³⁺-Catalyzed Cleavage of **4d.** To a glass vial containing 10 mL of methanol (93% deuterium content) were added **4d** (0.01 mmol), La(OTf)₃ (0.05 mmol), and NaOMe (0.05 mmol). The reaction mixture was left at room temperature for 4 h, after which it was concentrated to ~1 mL and the ¹H NMR spectrum (600 MHz) obtained. The spectrum indicated a mixture of 4-iodo methylsalicylate [δ 7.45 (1H, d, ArH, *J* = 8.58 Hz), 7.05 (1H, d, ArH, *J* = 1.41 Hz), 6.80 (1H, dd, ArH, *J* = 1.41, 8.32 Hz), 3.93 (<3H, s, OCH₃)] and trimethylphosphate [δ 3.73 (6H, d, P-(OCH₃)₂, *J* = 12 Hz)] containing a single CD₃O phosphoryl substituent. A ³¹P NMR (243.06 MHz) spectrum, referenced to 70% phosphoric acid, showed a single signal at 2.72 ppm.

f. Determination of Binding Constants. A general procedure was used to determine the conditional binding constant, K_{cond} , for phenol **4a** and La(OTf)₃ at pH 8.7 whereby a UV cuvette was charged with 18.4 mM *N*-*i*Pr-morpholine buffer containing 0.5 equiv of HClO₄ along with phenol **4a** (6.3×10^{-4} M) in 2.5 mL of methanol, and the spectrum from 250 to 400 nm was obtained. A 5 μL aliquot from a 55.5 mM La(OTf)₃ stock solution was added to the cell along with 1 equiv of NBu₄OCH₃ and another scan obtained. This procedure was repeated until the observed ΔAbs_{360} did not change, thereby indicating saturation binding. The change in total volume during titration of **3a** was approximately 2%. The K_{cond} was obtained by fitting of the $\Delta\text{Abs}_{360}^{\text{nm}}$ vs [La(OTf)₃] data to eq 5 (see Discussion).

g. Job Plot. To a series of UV cuvettes containing anhydrous methanol buffered with *N*-*i*Pr-morpholine (18.4 mM, containing 0.5 equiv of HClO₄) at pH 8.7 were added La(OTf)₃ and methyl 5-chlorosalicylate (phenol of **4c**) such that [La]_{total} + [phenol of **4c**] was maintained constant at 2.28 mM. A UV/vis spectrum was obtained on each sample scanning from 250 to 400 nm and the $\text{Abs}_{375}^{\text{nm}}$ plotted as a function of [phenol of **4c**]/([La]_{total} + [phenol of **4c**]) (see Supporting Information).

3. Results

a. Identification of Reaction Products. After 4 h, ¹H NMR analysis of the reaction mixture comprising 0.9 mM **4d**, 4.0 mM La(OTf)₃, and 4.0 mM NaOMe in CD₃OD/CH₃OH (93% deuterium content) indicated that the only observable products were trimethyl phosphate and methyl 4-iodosalicylate. Comparison of the aryl and the methoxycarbonyl proton intensities indicated that there was ~28% exchange of CO₂CH₃ for CO₂CD₃, which is due to the fact that the La³⁺ system promotes the transesterifications of carboxylate esters.²⁴ Phosphate triesters **4a–i** all underwent catalytic cleavage at pH 8.7 to produce the metal-bound aryl oxide complexes as the only identifiable products (>90% as determined by UV/vis spectrophotometry).

(22) (a) Neverov, A. A.; Liu, C. T.; Bunn, S. E.; Edwards, D.; White, C. J.; Melnychuk, S. A.; Brown, R. S. *J. Am. Chem. Soc.* **2008**, *130*, 6639. (b) Edwards, D. R.; Neverov, A. A.; Brown, R. S. *J. Am. Chem. Soc.* **2009**, *131*, 368.

(23) Padovani, M.; Williams, N. H.; Wyman, P. J. *Phys. Org. Chem.* **2004**, *17*, 472.

(24) (a) Neverov, A. A.; Sunderland, N. E.; Brown, R. S. *Org. Biomol. Chem.* **2005**, *3*, 65. (b) Neverov, A. A.; McDonald, T.; Gibson, G.; Brown, R. S. *Can. J. Chem.* **2001**, *79*, 1704.

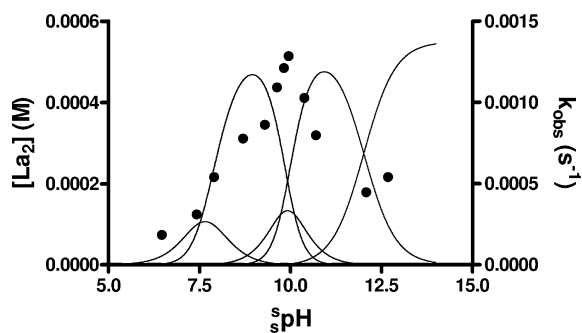


Figure 1. Plot of $[\text{La}^{3+}_2(\text{OCH}_3)_x]$ speciation (left axis) and k_{obs} (right axis) vs pH for the catalyzed methanolysis of **4a** (4.0×10^{-5} M) determined from the rate of appearance of product metal-bound phenoxide at 343 nm, $T = 25.0 \pm 0.1$ °C, and $[\text{La}(\text{OTf})_3]_{\text{total}} = 1.1$ mM.

Table 1. Kinetic Constants ($k_2^{2:x}$, $\text{M}^{-1} \text{s}^{-1}$) for the Methanolysis of **4a** Catalyzed by the Various $\text{La}^{3+}_2(\text{OCH}_3)_x$ Species Present at $[\text{La}^{3+}]_{\text{total}} = 1.1$ mM and $T = 25.0 \pm 0.1$ °C

	$\text{La}^{3+}_2(\text{OCH}_3)_x$				
	$x = 1$	$x = 2$	$x = 3$	$x = 4$	$x = 5$
$k_2^{2:x}$ ^a	2.74 (0.81)	1.11 (0.21)	5.81 (0.84)	1.10 (0.22)	0.75 (0.20)
$\text{p}K_{\text{a}}^{\text{La}}$ ^b		7.56 ^c	10.11 ^c	9.73 ^c	12.00 ^c

^a $k_2^{2:x}$ determined by fit of the k_{obs} vs pH data to eq 1 as described in the text. ^b $\text{p}K_{\text{a}}^{\text{La}}$ not calculable on the basis of the data at hand. ^c $\text{p}K_{\text{a}}^{\text{La}}$ for the hypothetical $\text{La}^{3+}_2(\text{OCH}_3)_x(\text{HOCH}_2)_n \leftrightarrow \text{La}^{3+}_2(\text{OCH}_3)_{x+1}(\text{HOCH}_2)_{n-1} + \text{H}^+$ ionization computed on the basis of potentiometric titration data given in ref 25.

b. pH/Rate Profile for the La^{3+} -Catalyzed Cleavage of Phosphate Ester **4a.** In Figure 1 is presented the $\text{La}^{3+}_2(\text{OCH}_3)_x/\text{pH}/\text{rate}$ profile for methanolysis of **4a** (4×10^{-5} M) promoted by $\text{La}(\text{OTf})_3$ (1.1 mM) as a function of varying amounts of added NBu_4OCH_3 . Figure 1 also includes the concentration dependencies of the various $\text{La}^{3+}_2(\text{OCH}_3)_x$ species^{10a,25} as a function of pH , which shows that the maximum rate of the catalyzed reaction loosely tracks the speciation profile for $\text{La}^{3+}_2(\text{OCH}_3)_3$ in solution. Closer analysis reveals that the other $\text{La}^{3+}_2(\text{OCH}_3)_x$ dimers also possess catalytic activity for the cleavage of **4a**. The pH/k_{obs} data were analyzed as a linear combination of the individual rate constants (eq 1),

$$k_{\text{obs}} = k_2^{2:1}[\text{La}^{3+}_2(\text{OCH}_3)_1] + k_2^{2:2}[\text{La}^{3+}_2(\text{OCH}_3)_2] + \dots + k_2^{2:x}[\text{La}^{3+}_2(\text{OCH}_3)_x] \quad (1)$$

where $k_2^{2:1}$, $k_2^{2:2}$, ..., $k_2^{2:x}$ are the second-order rate constants for the various $\text{La}_2(\text{OCH}_3)_{1,2,\dots,n}$ complexes. The $k_2^{2:x}$ constants listed in Table 1 indicate there is <10-fold difference in reactivity between all five complexes, with $\text{La}^{3+}_2(\text{OCH}_3)_3$ being the most reactive, having a computed $k_2^{2:3} = 5.81 \pm 0.84 \text{ M}^{-1} \text{ s}^{-1}$. Also given in Table 1 are the various $\text{p}K_{\text{a}}^{\text{La}}$ values for the formal $\text{La}^{3+}_2(\text{OCH}_3)_x(\text{HOCH}_2)_n \leftrightarrow \text{La}^{3+}_2(\text{OCH}_3)_{x+1}(\text{HOCH}_2)_{n-1} + \text{H}^+$ ionization computed from data given in ref 25. A Brønsted plot (Figure 14S, Supporting Information) of the $\log k_2^{2:x}$ data in Table 1 vs the $\text{p}K_{\text{a}}^{\text{La}}$ is fairly scattered, with a slope of $\beta_{\text{nuc}} = -0.02 \pm 0.15$.

c. Substituent Effects on the Rate of Reaction for the La^{3+} -Catalyzed Cleavage of Phosphate Esters **4a–i.** The rates of methanolyses of phosphate esters **4a–i** were investigated as a function of increasing $[\text{La}(\text{OTf})_3]$ at pH 8.7, $T = 25.0 \pm 0.1$

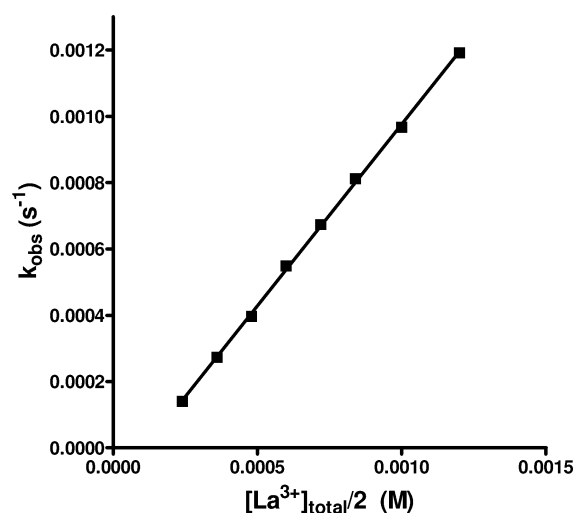


Figure 2. Plot of k_{obs} vs $[\text{La}]_{\text{total}}/2$ for the catalyzed methanolysis of **4a** (5×10^{-5} M) determined from the rate of appearance of product metal-bound phenoxide at 343 nm, $T = 25.0 \pm 0.1$ °C, pH 8.7. Linear regression of the data gives the second-order rate constants ($k_2^{\text{La}} = 1.10 \pm 0.01 \text{ M}^{-1} \text{ s}^{-1}$, $r^2 = 0.9995$).

°C. The Figure 1 speciation diagram indicates that, above 1 mM concentrations, all the metal ions exist as dimers at pH 8.7, with 92% being $\text{La}^{3+}_2(\text{OCH}_3)_2$ and the $\text{La}^{3+}_2(\text{OCH}_3)_1$ and $\text{La}^{3+}_2(\text{OCH}_3)_3$ species each accounting for about 4%. The reaction of **4a**, however, is readily shown to proceed 73% via $\text{La}^{3+}_2(\text{OCH}_3)_2$ and 12 and 15% respectively via the $\text{La}^{3+}_2(\text{OCH}_3)_1$ and $\text{La}^{3+}_2(\text{OCH}_3)_3$ complexes once one considers the rate constants for the species given in Table 1. We assume this is also the situation for each of **4b–i**. The linear k_{obs} vs $[\text{La}^{3+}]_{\text{total}}/2$ plot shown in Figure 2 for **4a** has an apparent x -intercept of $(1.10 \pm 0.07) \times 10^{-4}$ M. Nonlinear behavior in the plots of k_{obs} versus $[\text{La}^{3+}]_{\text{total}}/2$ has previously been observed at low concentrations for the La^{3+} -catalyzed methanolysis of neutral phosphate triesters¹⁰ and *N*-acetylimidazole.²⁶ These results were interpreted as being consistent with incomplete formation of the catalytically active $\text{La}^{3+}_2(\text{OCH}_3)_x$ dimeric complexes at $[\text{La}^{3+}]_{\text{total}}/2 < 1.5 \times 10^{-4}$ M, which is assumed to be the case in the current study. Plots of k_{obs} versus $[\text{La}^{3+}]_{\text{total}}/2$ for all substrates **4b–i** are similar in appearance to that shown in Figure 2. The second-order rate constants (k_2^{La}) were determined as the slopes of their linear plots and are listed in Table 2.

Given in Figure 3 are the Brønsted plots of $\log k_2^{\text{La}}$ vs $\text{p}K_{\text{a}}^{\text{Lg}}$ for the La^{3+} -promoted cleavage of **4a–i** and, for comparison purposes, the La^{3+} -catalyzed methanolysis of substrates **3a,b,d,e**, where the two slopes are $\beta_{\text{lg}}^{\text{La}} = -0.82$ and $\beta_{\text{lg}}^{\text{La}} = -1.25$. The Brønsted plot of $\log k_2^{\text{OMe}} vs \text{p}K_{\text{a}}^{\text{Lg}}$ for the cleavage of **4a,b,d,e,f,h** fits a linear regression of $\log k_2^{\text{OMe}} = (-0.51 \pm 0.04)\text{p}K_{\text{a}}^{\text{Lg}} + (4.68 \pm 0.56)$. Not shown in Figure 3 for reasons of visual clarity is the Brønsted plot of $\log k_2^{\text{OMe}} vs \text{p}K_{\text{a}}^{\text{Lg}}$ for the methoxide-catalyzed cleavage of **3a–e**, which fits a standard linear regression of $\log k_2^{\text{OMe}} = (-0.59 \pm 0.07)\text{p}K_{\text{a}}^{\text{Lg}} + (5.41 \pm 0.91)$. The substituents on the aryl ring of **4** influence the reactivity by interactions with both the *o*-CO₂Me group and the bridging phenoxy oxygen during the La^{3+} -promoted P–OAr bond cleavage. Attempts to correlate the k_2^{La} for methanolysis

(25) Gibson, G. T. T.; Neverov, A. A.; Brown, R. S. *Can. J. Chem.* **2003**, *81*, 495.

(26) Neverov, A. A.; Montoya-Pelaez, P.; Brown, R. S. *J. Am. Chem. Soc.* **2001**, *123*, 210.

(27) Bunn, S. E.; Liu, C. L.; Lu, Z.-L.; Neverov, A. A.; Brown, R. S. *J. Am. Chem. Soc.* **2007**, *129*, 16238.

Table 2. Second-Order Rate Constants k_2^a and k_2^{OMe} Determined for the Methoxide- and $\text{La}(\text{OTf})_3$ -Catalyzed Cleavage of **4a–i** and **3a–e**

substrate	$\text{p}K_a^{\text{phenol}}$	k_2^a (M ⁻¹ s ⁻¹)	k_2^{OMe} (M ⁻¹ s ⁻¹)
4a	14.20	1.10 ± 0.01	(3.20 ± 0.02) × 10 ⁻³
4b	10.64	(6.98 ± 0.34) × 10 ²	(1.69 ± 0.04) × 10 ⁻¹
4c	12.57	(1.29 ± 0.05) × 10 ¹	
4d	12.79	(5.50 ± 0.16) × 10 ¹	(1.79 ± 0.07) × 10 ⁻²
4e	13.20	2.23 ± 0.04	(5.91 ± 0.02) × 10 ⁻³
4f	13.24	(1.42 ± 0.08) × 10 ¹	(1.18 ± 0.04) × 10 ⁻²
4g	14.50	1.16 ± 0.03	
4h	14.65	(1.21 ± 0.03) × 10 ⁻¹	(1.39 ± 0.06) × 10 ⁻³
4i	14.82	(5.01 ± 0.17) × 10 ⁻¹	
3a	10.73	(9.25 ± 0.20) × 10 ²	(1.30 ± 0.01) × 10 ⁻¹
3b	11.18	(1.28 ± 0.92) × 10 ²	(4.48 ± 0.03) × 10 ⁻²
3c	12.41		(2.58 ± 0.03) × 10 ⁻²
3d	13.59	(2.50 ± 0.42) × 10 ⁻¹	(3.12 ± 0.06) × 10 ⁻³
3e	14.33	1.86 × 10 ⁻²	(6.29 ± 0.14) × 10 ⁻⁴

^a Determined from linear regression of the plots of k_{obs} vs $[\text{La}^{3+}]_{\text{total}}/2$ at pH 8.7, $T = 25.0 \pm 0.1$ °C. ^b Determined from linear regression of the plots of k_{obs} vs $[\text{NaOCH}_3]$ at $T = 25.0 \pm 0.1$ °C.

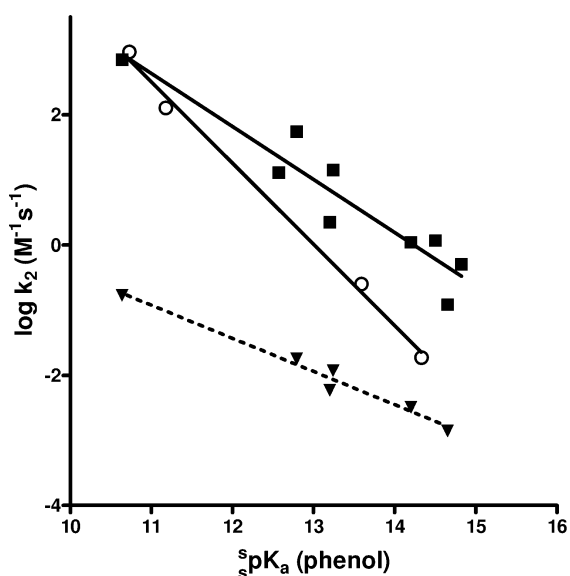


Figure 3. Brønsted plots for the La^{3+} -catalyzed methanolysis of phosphate triesters **4** (■, solid line) determined at pH 8.7, $T = 25.0 \pm 0.1$ °C, where $\log k_2^a = (-0.82 \pm 0.11)\text{p}K_a^{\text{phenol}} + (11.61 \pm 1.48)$, $r^2 = 0.8878$, nine data; the La^{3+} -catalyzed methanolysis of substrates **3** (○, solid line), where $\log k_2^a = (-1.25 \pm 0.06)\text{p}K_a^{\text{phenol}} + (16.23 \pm 0.75)$, $r^2 = 0.9954$, four data; and the methoxide-catalyzed methanolysis of phosphate triesters **4** (▲, dashed line), where $\log k_2^{\text{OMe}} = (-0.51 \pm 0.04)\text{p}K_a^{\text{phenol}} + (4.68 \pm 0.56)$, $r^2 = 0.9730$, six data. For visual clarity, the Brønsted plot for the methoxide-catalyzed methanolysis of phosphate triesters **3** is not shown; however, a fit of the data provided in Table 2 gives $\log k_2^{\text{OMe}} = (-0.59 \pm 0.07)\text{p}K_a^{\text{phenol}} + (5.41 \pm 0.91)$, $r^2 = 0.9557$, five data.

of **4a–i** using a single substituent parameter as in a standard Brønsted or Hammett plot resulted in the apparent scattering of the data depicted in Figure 3. In addition, when the rate constants pertaining to cleavage of **4a–i** were fit to a two-parameter model using the Jaffé equation,

$$\log(k_2^x/k_2^{\text{H}}) = \rho_{\text{phosphate}} \sigma^{\text{phosphate}} + \rho_{\text{C(O)OMe}} \sigma^{\text{C(O)OMe}} \quad (2)$$

where $\sigma^{\text{phosphate}}$ and $\sigma^{\text{C(O)OMe}}$ refer to the sigma substituent constants as they relate to the bridging oxygen and *o*- CO_2Me substituents of the aryloxy leaving group, respectively, incon-

sistent results were obtained which depended upon the method of fitting employed (see Supporting Information for a complete discussion).

d. Determination of Binding Constants (K_b) for Phenoxide Leaving Groups **4a,c–i.** Binding constants for the parent phenols of phosphates **4a,c–i** with $\text{La}(\text{OTf})_3$ were determined by spectrophotometric titrations at pH 8.7. In Figure 4a is the $\Delta\text{Abs}^{375 \text{ nm}}$ vs $[\text{La}^{3+}]$ plot for the titration of methyl 5-chlorosalicylate (parent phenol of **4c**), where the calculated line is obtained by fitting the data to eq 3,

$$\text{Abs}_{\text{obs}} = \text{Abs}_{\text{max}}(1 + K_{\text{cond}}[\text{Sub}] + [\text{La}]K_{\text{cond}} - X)/(2K_{\text{cond}})/[\text{Sub}] \quad (3)$$

where

$$X = (1 + 2K_{\text{cond}}[\text{Sub}] + 2[\text{La}]K_{\text{cond}} + K_{\text{cond}}^2[\text{Sub}]^2 - 2K_{\text{cond}}^2[\text{La}][\text{Sub}] + [\text{La}]^2K_{\text{cond}}^2)^{0.5}$$

which generates a conditional binding constant, K_{cond} , of $(5.0 \pm 0.9) \times 10^4 \text{ M}^{-1}$ that corresponds to the process shown in Scheme 1. Shown in Figure 4b is the $\text{Abs}^{302 \text{ nm}}$ versus $[\text{La}^{3+}]$ plot for the titration of 4-chlorophenol. Its K_{cond} is $(4.4 \pm 0.3) \times 10^2 \text{ M}^{-1}$, indicating that this phenol, without the *o*- CO_2Me group, binds to the La^{3+} complex(es) much more weakly than does methyl 5-chlorosalicylate. The binding constants, K_b , for all species are calculated using eq 4, as reported in a related study,^{22b} using the K_{cond} values, the $\text{p}K_a^{\text{phenol}}$ values for each phenol, and the $[\text{H}^+]$ corresponding to the pH at which the spectroscopic titrations were performed.

$$K_b = \frac{[\text{H}^+]K_{\text{cond}}}{K_a} \quad (4)$$

Table 3 gives the K_{cond} and K_b values determined for the parent phenols of phosphates **4a,c–i**. A Brønsted plot (Figure 5) of $\log K_b$ vs $\text{p}K_a^{\text{phenol}}$ of the phenol gives a regression of $\log K_b = (0.85 \pm 0.07)\text{p}K_a^{\text{phenol}} - (2.1 \pm 1)$. Binding constants were also determined for phenols not possessing the *o*- CO_2Me substituent in order to quantify the stabilization afforded to the binding of La^{3+} by that group (see Table 3, entries 9–12). These data fit a linear regression of $\log K_b = (0.49 \pm 0.06)\text{p}K_a^{\text{phenol}} - (0.71 \pm 0.74)$.

A Job plot of $\text{Abs}^{375 \text{ nm}}$ versus $[\text{phenol of } \mathbf{4c}]/([\text{La}^{3+}]_{\text{total}} + [\text{phenol of } \mathbf{4c}])$ (total concentration = 2.28 mM) is shown in the Supporting Information, Figure S13. The plot has a plateau maximum from 0.5 to 0.66, showing that at these concentrations the La^{3+}_2 dimer system binds 2–3 molecules of the phenoxide.

4. Discussion

a. pH vs k_2^a Profile. The speciation/rate constant plot in Figure 1 for the cleavage of **4a** is reminiscent of that for La^{3+} -catalyzed methanolysis of paraoxon,^{10a} where there is also a non-integer slope in the $\log k_2^a$ vs pH plot. This sort of plot for metal-methoxide-catalyzed reactions results from the effectiveness of catalysis of the different metal–methoxy forms, the speciation and concentrations of which change with pH .²⁸ All the $\text{La}^{3+}_2(\text{OCH}_3)_x$ ($x = 1–5$) species formed over the pH range of this study show some catalytic activity, with the

(28) Gibson, G. T. T.; Neverov, A. A.; Teng, A. C.-T.; Brown, R. S. *Can. J. Chem.* **2005**, *83*, 1268.

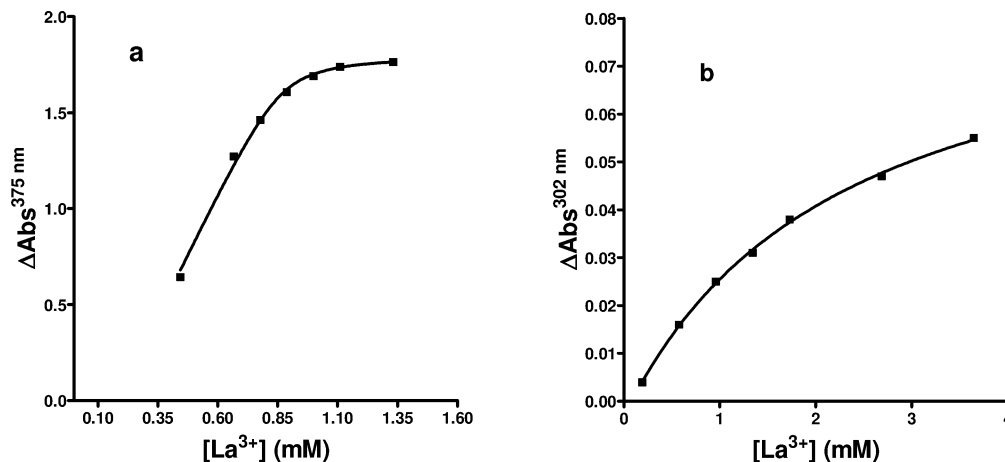


Figure 4. (a) Plot of $\Delta\text{Abs}^{375\text{ nm}}$ versus $[\text{La}(\text{OTf})_3]$ for the spectrophotometric titration of methyl 5-chlorosalicylate at §pH 8.7 and 25.0 ± 0.1 °C; fit of the data to eq 3 gives $K_{\text{cond}} = (5.0 \pm 0.9) \times 10^4 \text{ M}^{-1}$. (b) Plot of $\Delta\text{Abs}^{302\text{ nm}}$ versus $[\text{La}(\text{OTf})_3]$ for the spectrophotometric titration of 4-chlorophenol at §pH 8.7 and 25.0 ± 0.1 °C; fit of the data to eq 4 gives $K_{\text{cond}} = (4.4 \pm 0.3) \times 10^2 \text{ M}^{-1}$.

Scheme 1. Thermodynamic Cycle for the $\text{La}(\text{OTf})_3$ Binding of the Phenol Corresponding to **4a**

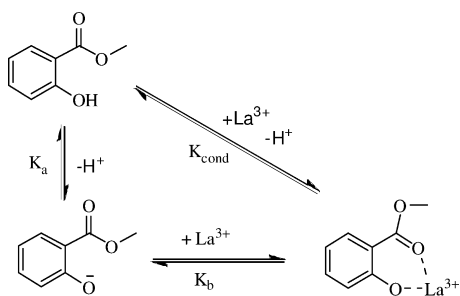


Table 3. K_{cond} and K_b Binding Constants for the Complexation of Phenols Corresponding to Phosphates **4a,c–i** with La^{3+} , Determined by Spectrophotometric Titration at §pH 8.7 and $T = 25$ °C

phenol corresponding to parent phosphate	K_{cond}^b ($\times 10^4 \text{ M}^{-1}$)	K_b^c (M^{-1})
4a	$(2.6 \pm 0.6) \times 10^4$	7.4×10^9
4c	$(5.0 \pm 0.9) \times 10^4$	3.7×10^8
4d	$(6.6 \pm 1.3) \times 10^4$	7.5×10^8
4e	$(4.1 \pm 1.7) \times 10^4$	1.2×10^9
4f	$(8.6 \pm 1.1) \times 10^4$	2.7×10^9
4g	$(2.2 \pm 0.4) \times 10^4$	1.3×10^{10}
4h	$(4.4 \pm 0.8) \times 10^4$	3.9×10^{10}
4i	$(3.6 \pm 0.5) \times 10^4$	4.3×10^{10}
2-chloro-4-nitrophenol ^d	$(3.6 \pm 0.1) \times 10^4$	1.6×10^5
3-methyl-4-nitrophenol ^d	$(3.8 \pm 0.2) \times 10^3$	2.4×10^6
4-chlorophenol ^d	$(4.4 \pm 0.3) \times 10^2$	3.4×10^7
3-methoxyphenol ^d	$(1.1 \pm 0.1) \times 10^2$	1.9×10^7

^a Protocols for the determination of $\text{§p}K_{\text{a}}^{\text{phenol}}$ in methanol described in the Experimental Section. ^b Determined by fitting ΔAbs versus $[\text{La}(\text{OTf})_3]$ data to eq 4. ^c Calculated with eq 5 as described in the text. ^d The $\text{§p}K_{\text{a}}^{\text{phenol}}$ data can be found in refs 22a and 27.

$\text{La}^{3+}_2(\text{OCH}_3)_3$ complex having the largest rate constant of $k_2^{2:3} = 5.8 \pm 0.8 \text{ M}^{-1} \text{ s}^{-1}$. However, the $k_2^{2:x}$ values are relatively insensitive to the large variation in the $\text{§p}K_{\text{a}}$ values for the $\text{La}^{3+}_2(\text{OCH}_3)_x$ species, as is revealed in the Brønsted plot, where the $\beta_{\text{nuc}} = -0.02$. Low values for β_{nuc} are often observed for metal–hydroxo complexes attacking C=O-containing species.²⁹ It was reported that the reaction of some mononuclear metal–hydroxo complexes exhibited a β_{nuc} of 0.43 ± 0.13 in their reaction with diethyl 2,4-dinitrophenyl phosphate, although

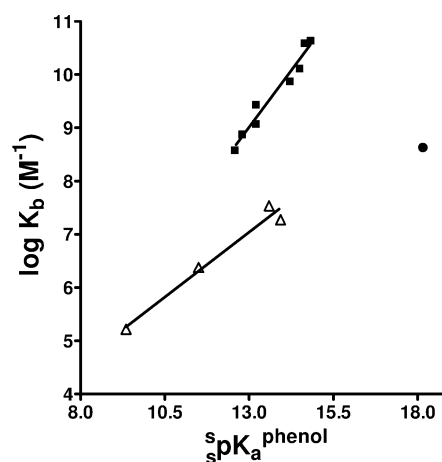


Figure 5. Plot of $\log K_b$ vs $\text{§p}K_{\text{a}}^{\text{phenol}}$ for the parent phenols of **4a,c–i** (■) which fit a linear regression of $\log K_b = (0.85 \pm 0.07)\text{§p}K_{\text{a}}^{\text{phenol}} - (2.1 \pm 1)$, $r^2 = 0.959$, eight data, and for phenols lacking the *o*-CO₂Me substituent (△) which fit a linear regression of $\log K_b = (0.49 \pm 0.06)\text{§p}K_{\text{a}}^{\text{phenol}} - (0.71 \pm 0.74)$, $r^2 = 0.970$, four data. (●) Binding constant for methoxide ($\text{§p}K_{\text{a}}^{\text{methanol}} = 18.16$) coordination to $\text{La}_2(\text{OMe})_1$ forming the 2:2 complex of $\text{La}_2(\text{OMe})_2$.

the cleavage mechanism was claimed to be a general base one in contrast to the more complicated nucleophilic one believed operative here with the La^{3+} dimers.³⁰ More pertinent to the discussion is the finding that a homologous series of five mononuclear Zn(II) triamine complexes catalyze the hydrolysis of diethyl 2,4-dinitrophenyl phosphate with a β_{nuc} of -0.15 ± 0.01 by a proposed nucleophilic mechanism involving Lewis acid activation of the substrate and intramolecular attack of the coordinated hydroxide.³¹ The low value of the β_{nuc} found in the current study is reasonably suggested to result from a complex combination of competing effects of increased nucleophilicity for the methoxide attached to the species with the highest $\text{§p}K_{\text{a}}$ values, coupled with a concomitant decreasing Lewis acidity/electrophilic activation and LGA attributable to the reduced net positive charge on the two La^{3+} ions in the complex.

b. Binding of Aryl Oxides to La^{3+} . The general appearance of the representative Abs vs $[\text{La}^{3+}]$ plots in Figure 4a,b

(30) Hay, R. W.; Govan, N. *Trans. Met. Chem.* **1998**, *23*, 133.

(31) Itoh, T.; Tada, T.; Yoshikawa, Y.; Hisada, H. *Bull. Chem. Soc. Jpn.* **1996**, 1265.

(29) Martin, R. B. *J. Inorg. Nucl. Chem.* **1976**, *38*, 511.

determined for the parent phenols of **3d** and **4c** indicates the *o*-CO₂Me substituent provides enhanced binding to the metal complex relative to phenols without this group. The appearance of the spectrophotometric titration plots with a slight *x*-intercept and steep slope is consistent with a process wherein the aryl oxides corresponding to phosphates **4a,c–i** bind to one or more dimeric La³⁺ forms. The Job plot (Supporting Information) further indicates that 2–3 aryl oxides can be accommodated at equilibrium within the coordination sphere of the dimeric La³⁺₂(⁻OCH₃)_{*x*} complex to give a bound form of stoichiometry La³⁺₂(⁻OAr)_{2–3}(⁻OCH₃)_{*x*}.

The metal-bound aryl oxide complexes are the only observable aryloxy products from the catalytic cleavage of **4a–i** at pH 8.7 (>90% by UV/vis spectrophotometry). At the pH where these reactions were run, the complete binding of the aryl oxide anion indicates that the $\text{p}K_{\text{a}}$ for the parent phenol of **4a** is reduced by at least 6.5 pH units by complexation to La³⁺₂(⁻OCH₃)_{*x*} (Scheme 1). At pH 8.7 and 1.1 mM La(OTf)₃, the speciation diagram of Figure 1 indicates that all the metal ions exist as dimers, with 92% being La³⁺₂(⁻OCH₃)₂, while La³⁺₂(⁻OCH₃)₁ and La³⁺₂(⁻OCH₃)₃ account for about 4% each. The gross binding constants (*K*_b) for the aryl oxides corresponding to **4a,c–i** with the La³⁺-containing species present at that pH are listed in Table 3: the values are large and range from 4×10^8 to $4 \times 10^{10} \text{ M}^{-1}$.

The slope of 0.85 for the plot of log *K*_b versus the $\text{p}K_{\text{a}}$ values of the phenols with the *o*-CO₂Me groups (Figure 5) is experimentally identical to that found for Yb³⁺ complexation of these same phenoxides in methanol (0.84).^{22b} This value indicates that a formal charge of approximately –0.15 resides on the oxyanion in the metal-bound complex and suggests that 85% of the negative charge is acquired by the metal complex on binding the phenoxide to the La³⁺₂(⁻OCH₃)_{*x*}. Aryl oxides without the *o*-CO₂Me substituent also bind to the La³⁺₂(⁻OCH₃)_{*x*} species, albeit with significantly smaller *K*_b constants (Table 3, entries 9–12). The log *K*_b vs $\text{p}K_{\text{a}}$ plot in Figure 5 has a slope of 0.49, indicating that these phenoxides experience a lesser degree of charge neutralization upon La³⁺ complexation and so have a formal charge of –0.5 residing on the coordinated aryl oxides. An estimation of the enhanced stability afforded the La³⁺–aryl oxide complexes by the *o*-CO₂Me group is possible based on an extrapolation of the lower line of Figure 5 to a $\text{p}K_{\text{a}}$ of 14.20, which corresponds to a phenol having $\text{p}K_{\text{a}}$ identical to that of 2-(methoxycarbonyl)phenol but lacking the *ortho*-substitution. The extrapolated *K*_b of $4.7 \times 10^7 \text{ M}^{-1}$ indicates that the *o*-CO₂Me group provides an additional stabilization of ~3 kcal/mol.

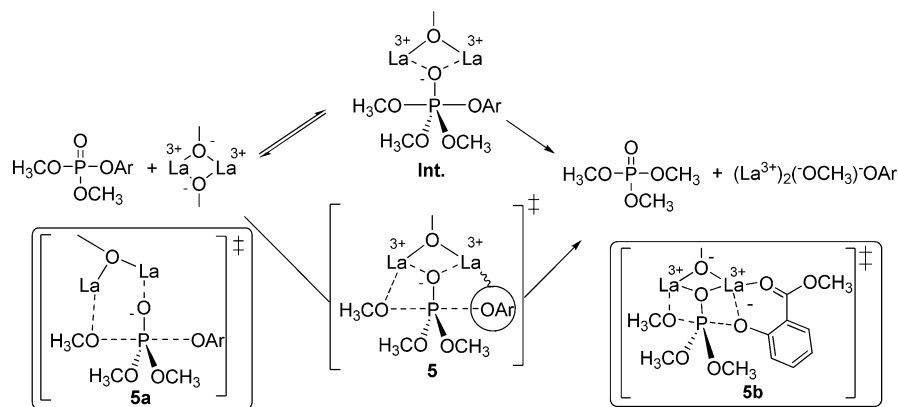
c. Linear Free Energy Treatment of the Rate Data. The *k*₂^{1a} values for La³⁺-catalyzed cleavage of **4a–i** listed in Table 2 vary by nearly a factor of 6000. These give a rather scattered Brønsted plot (Figure 3) with a best fit of $\log k_2^{1a} = (-0.82 \pm 0.11)\text{p}K_{\text{a}}^{\text{lg}} + (11.31 \pm 1.48)$. The β_{lg} of –0.82 is less than that determined for the same sort of plot for the La³⁺-catalyzed cleavage of phosphates **3** ($\beta_{\text{lg}} = -1.25$). While at first glance this may suggest that P–OAr cleavage in the reaction of **4a–i** is less extensive than with substrates **3**, other evidence (*vide infra*) indicates that cleavage is well advanced with **4a–i**, and the less negative β_{lg} value is consistent with La₂³⁺(⁻OCH₃)_{*x*} assistance of leaving group departure. In our previous study^{10c} on the La³⁺-catalyzed methanolysis of diethyl aryl phosphate esters, a β_{lg} of –1.43 was determined which, in consideration of the associated error limits, is experimentally identical to the β_{lg} of –1.25 determined here for substrates **3**.

The *k*₂^{0Me} values for the methoxide-catalyzed cleavage of **4** listed in Table 2 differ by only ~10². The Brønsted plot of these data fits a linear regression of $\log k_2^{0\text{Me}} = (-0.51 \pm 0.04)\text{p}K_{\text{a}}^{\text{lg}} + (4.68 \pm 0.56)$, whereas that for the methoxide reaction of phosphates **3** is $\log k_2^{0\text{Me}} = (-0.59 \pm 0.07)\text{p}K_{\text{a}}^{\text{lg}} + (5.41 \pm 0.91)$. Given the error limits, the two β_{lg} values of –0.51 and –0.59 are close enough to suggest that the extent of P–OAr bond rupture in the TSs for the two series is essentially identical. The amount of bond rupture is calculated to be 27–32% based on the Leffler parameter,³² $\alpha = \beta_{\text{lg}}/\beta_{\text{eq}}$, where the β_{eq} of –1.87 pertains to the equilibrium transfer of the diethoxyphosphoryl group between oxyanion nucleophiles in water,³³ which we assume is similar to the situation in methanol.

d. Mechanistic Possibilities for the Catalyzed Reaction. The mechanism of the La³⁺-catalyzed^{10c} methanolysis and oxyanion-promoted cleavage^{15,33} of phosphate triesters has been discussed considering stepwise or concerted reactions. For acyclic phosphotriesters with aryloxy leaving groups, linear free energy data support concerted reactions for oxyanion nucleophiles, with the TSs being looser for leaving groups with low *pK*_a's and tighter with poorer leaving groups.³³ Stepwise mechanisms for the reaction of phosphate esters have also been proposed and demonstrated convincingly in some instances, generally with six-membered cyclic phosphates.³⁴

For metal-ion-catalyzed cleavage of phosphate triesters, there is little literature guidance about concerted or stepwise cleavage, although we have previously favored concerted processes for methanolyses of diethyl aryl phosphates promoted by both La³⁺ and a Zn(II) complex, primarily because of the large degree of P–OAr cleavage ($\beta_{\text{lg}} = -1.43$ and –1.12, respectively).^{10c} At one limit, the La³⁺-catalyzed methanolysis of phosphate esters **4a–i** might follow a stepwise reaction mechanism (A_N + D_N) as in Scheme 2, although the very large β_{lg} found with substrates **3** without a *o*-CO₂Me group might require that the rate-limiting step is breakdown of the intermediate.^{35,36} The Brønsted β_{lg} of –0.82 for the *o*-CO₂Me-containing phosphates **4** could also be consistent with this process. A rate-limiting breakdown of the intermediate would require a fast and reversible addition of the nucleophile to **4** that might be detected by an isotopic exchange experiment conducted in CD₃OD. However, no incorporation of a CD₃O⁻ group into unreacted **4** was detected for the La³⁺-catalyzed reaction of **4d** in methanol-*d*₄, even though the exclusive P-containing product is CD₃O–P(O)(OCH₃)₂. This experiment is suggestive, but the exchange via a phosphorane intermediate must involve one OCH₃ group at an apical position

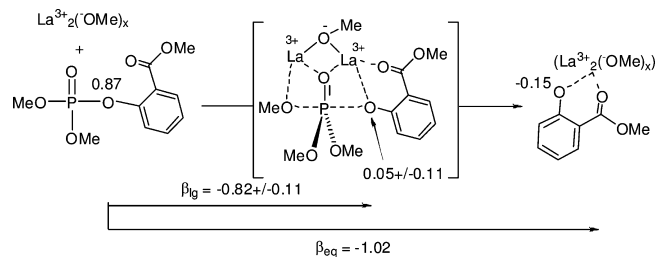
- (32) (a) Leffler, J. E.; Grunwald, E. *Rates and equilibria of organic reactions*; Wiley: New York, 1963. (b) Williams, A. *Acc. Chem. Res.* **1984**, *17*, 425.
- (33) (a) Ba-Saif, S. A.; Williams, A. *J. Org. Chem.* **1988**, *53*, 2204. (b) Ba-Saif, S. A.; Waring, M. A.; Williams, A. *J. Am. Chem. Soc.* **1990**, *112*, 8115. (c) Ba-Saif, S. A.; Waring, M. A.; Williams, A. *J. Chem. Soc. Perkin Trans 2* **1991**, 1653.
- (34) (a) Bromilow, R. H.; Khan, S. A.; Kirby, A. J. *J. Chem. Soc., Perkin Trans. 2* **1972**, 911. (b) Assad, N.; Kirby, A. J. *J. Chem. Soc., Perkin Trans. 2* **2002**, 1708. (c) Hall, C. R.; Inch, T. D. *Tetrahedron* **1980**, *36*, 2059. (d) Khan, S. A.; Kirby, A. J. *J. Chem. Soc. B* **1970**, 1172. (e) Rowell, R.; Gorenstein, D. G. *J. Am. Chem. Soc.* **1981**, *103*, 5894.
- (35) An analogous situation arises in the di-Co(III) complex promoted cleavage of some methyl aryl phosphates in water, where a very large β_{lg} of –1.38 for intramolecular attack of a di-Co(III)-coordinated oxide on the P was originally interpreted as arising from a concerted process with a late transition state,^{36a} but later shown that the more likely pathway had two steps with rate-limiting breakdown of the intermediate.^{36b}
- (36) (a) Williams, N. H.; Cheung, W.; Chin, J. *J. Am. Chem. Soc.* **1998**, *120*, 8079. (b) Humphrey, T.; Forconi, M.; Williams, N. H.; Hengge, A. C. *J. Am. Chem. Soc.* **2004**, *126*, 11864.

Scheme 2. Hypothetical Stepwise A_N + D_N and Concerted A_ND_N Mechanisms for La³⁺₂(-OCH₃)₂-Catalyzed Cleavage of **3** and **4**

during its formation or, alternatively, pseudorotation^{15,37} of the first-formed phosphorane and translocation of La³⁺ to provide assistance of OCH₃ departure. The pseudorotation, if required, could be too slow to be permitted by a short-lived intermediate.³⁸

A concerted (A_ND_N) reaction mechanism for the La³⁺-catalyzed cleavage of substrates **3** and **4** is also depicted in Scheme 2 as the lower pathway and involves electrophilic activation of the ester through P=O...La³⁺ coordination, delivery of a metal-coordinated methoxide, and extensive departure of the leaving group. In an earlier study^{10c} on the cleavage of diethyl aryl phosphate esters, we suggested that it was unlikely that an alkoxide (or hydroxide) bound between two metal ions would be sufficiently nucleophilic to attack the P=O unit, so that the La³⁺₂(-OCH₃)₂ dimer opens to give a terminally coordinated methoxide along with the P=O unit being bound to the second La³⁺, such as in TS **5a**. The only difference between that TS and the hypothetical TS **5** shown in Scheme 2 involves a slight movement of the metal ions to provide double coordination of the O=P during the concerted process. With phosphates **3** the departing group is not coordinated to La³⁺, but there could be a strong electrostatic interaction that does not involve extensive charge transfer from -OAr to the La³⁺ but is consistent with the large observed β_{lg}. The reduced β_{lg} observed with **4** might be explained in terms of TS **5b**, where the net charge buildup on the departing group is reduced by some coordinative association with La³⁺. Additional evidence for leaving group assistance in the La³⁺-catalyzed cleavage of phosphate esters **4a–i** is presented in the following section.

e. Catalysis Involving Leaving Group Assistance. Aspects of the current study with **4a–i** resemble those observed for the Yb³⁺-catalyzed reaction of phosphate diesters with the same series of leaving groups^{22b} as well as with a di-Zn(II) complex-catalyzed reaction of some methyl aryl phosphates.^{22a} There are three main similarities: (1) The reaction products for the La³⁺-catalyzed cleavage of **4a–i** are the metal-bound aryl oxides, as is the case in the Yb³⁺ and dinuclear Zn(II) complex-catalyzed reactions. The linear regressions of the log K_b vs $\text{p}K_{\text{a}}^{\text{phenol}}$ plots shown in Figure 5 point to an additional ~3 kcal/

Scheme 3. Charge Map for the La³⁺₂(-OCH₃)_x-Catalyzed Methanolysis of **4a**

mol of stabilization for binding the La³⁺₂(-OCH₃)_x to the parent phenoxide of **4a** relative to a phenol of identical $\text{p}K_{\text{a}}$ but lacking the *o*-CO₂Me substituent. (2) Substrates bearing the *o*-CO₂Me substituent undergo La³⁺-catalyzed cleavage at a significantly higher rate than substrates not having that group. In the case of substrate **4a**, this amounts to a 60-fold acceleration relative to **3e**, which is similar to the acceleration seen with diesters cleaved by the di-Zn(II) complex in methanol^{22a} but not nearly as large as the 10¹² seen for the Yb³⁺-promoted reactions of diesters.^{22b} Interestingly, the additional catalysis achieved with substrates **4** relative to **3** is more efficient for poorer leaving groups, as can be clearly seen upon visual inspection of the Brønsted plots (Figure 3). The best leaving groups from each series, **4a** and **3a**, essentially lie at the point of intersection of the two Brønsted plots, which suggests that with leaving groups of $\text{p}K_{\text{a}}^{\text{phenol}}$ less than ~10.7, catalysis involving leaving group assistance is no longer a requirement or even beneficial. (3) The Brønsted β_{lg} observed for cleavage of **4** in this study (-0.82) is shallower than the -1.25 determined for the analogous reaction with substrates **3**. This feature is also noted for the di-Zn(II) complex-catalyzed cleavage of phosphate diesters having the *o*-CO₂Me group.^{22a} We can construct the charge map shown in Scheme 3 for the reaction of **4a** with La³⁺₂(-OCH₃)_x, assuming that the starting P-OAr bridging oxygen has a charge of +0.87.³³ Insofar as the aqueous values are relevant to the situation in methanol, the effective charge residing on the La³⁺₂(-OCH₃)_x-bound phenoxide is calculated as EC_{ArOLa} = EC_{ArO⁻} + β_{bind} = -1.0 + (0.85) = -0.15, where the value of 0.85 comes from the plot in Figure 5, log K_b = (0.85 ± 0.07) $\text{p}K_{\text{a}}$ - (2.1 ± 1). The nascent cleaved phenoxy species cannot be exactly the same as what is formed in the equilibrium binding experiments of phenol plus La³⁺₂(-OCH₃)_x used to determine the K_b values for Figure 5. Thus, the computed EC_{ArOLa} value of -0.15 only provides a lower estimate for the β_{eq} of -1.02 and an upper estimate for the charge of 0.05 ± 0.11 on the leaving group in

(37) (a) Westheimer, F. H. *Acc. Chem. Res.* **1968**, *1*, 70. (b) Thatcher, G. R.; Kluger, R. *Adv. Phys. Org. Chem.* **1989**, *25*, 99.

(38) The requirement that departure of the aryloxy leaving group is rate limiting at first seems odd, given that its departure would be slower than that of the methoxide nucleophile, even though the $\text{p}K_{\text{a}}$ values for all the ArylOH groups of **4** are considerably lower than that of methanol (18.2). However, the metal-catalyzed reaction promoted by La³⁺₂(-OCH₃)₂ proceeds via a La³⁺-coordinated methoxide, the $\text{p}K_{\text{a}}$ of which is 7.56 (Table 1), meaning that the metal-coordinated methoxide is actually the better leaving group.

Table 4. Activation Parameters for the Lyoxide- and La^{3+} -Promoted Cleavage of Dimethyl Paraoxon and **4a**

reaction	ΔH^\ddagger (kcal/mol)	ΔS^\ddagger (cal/mol·K)	ΔG_{25}^\ddagger (kcal/mol)
DMP + ^-OMe	14.7 ± 0.7	-16.0 ± 2	19.5
DMP + $^-\text{OH}^a$	11.6	-26	19.3
DMP + ^-OH (calc) ^b	11.6	-31.9	21.1
(DMP + La^{3+}) ^c	0.70 ± 0.05	-46.5 ± 0.2	14.6
4a + ^-OMe	15.6 ± 0.3	-17.4 ± 0.95	20.8
4a + La^{3+} ^d	3.3 ± 0.1	-47.0 ± 0.4	17.3

^a Reference 40. ^b Reference 42. ^c Determined at $[\text{La}(\text{OTf})_3]_{\text{total}} = 2.0$ mM, $\text{pH} = 9.1$, ref 39. ^d Determined at $[\text{La}(\text{OTf})_3]_{\text{total}} = 1.5$ mM, $\text{pH} = 8.7$.

the TS. Although an estimate, the calculation indicates that the Leffler index (α) of 0.80 ± 0.10 for the cleavage of the P–OAr bond in the methanolyse of **4** is experimentally indistinguishable from that found for the La^{3+} -catalyzed cleavages of **3**, where $\alpha = \beta_{\text{lg}}/\beta_{\text{eq}} = -1.25 \pm 0.06/1.87 = 0.67 \pm 0.06$. Thus, the decreased β_{lg} determined for the reaction of substrates **4** is not a result of less P–OAr bond rupture but rather a manifestation of the reduction in total charge development at the bridging oxygen as a result of metal-ion-mediated leaving group assistance.

f. Activation Parameters for the La^{3+} - and $^-\text{OCH}_3$ -Promoted Cleavage of Some Phosphate Triesters. The activation parameters for the $^-\text{OCH}_3$ - and La^{3+} -promoted reactions of dimethyl paraoxon ($(\text{CH}_3\text{O})_2\text{P}(=\text{O})\text{-OC}_6\text{H}_4\text{NO}_2$, DMP)³⁹ and **4a** are given in Table 4. The data for the methoxide reaction of DMP are similar to the activation parameters obtained experimentally for the hydroxide-promoted reaction in water,^{40,41} and a recent report gives computed values for the hydroxide reaction of 11.6 kcal/mol, -31.9 cal/mol·K, and 21.1 kcal/mol for the ΔH^\ddagger , ΔS^\ddagger , and ΔG_{25}^\ddagger for which the TS was said to comprise an in-line concerted process with little cleavage of the departing *p*-nitrophenoxy group.⁴² The β_{lg} value of -0.51 for the $^-\text{OCH}_3$ reaction of series **4** is also consistent with a concerted reaction where the Leffler parameter indicates $\sim 30\%$ P–OAr bond cleavage in the TS.

The La^{3+} -catalyzed methanolyse for DMP and **4a** have very low ΔH^\ddagger values that are compensated by large negative ΔS^\ddagger terms, as might be expected for a TS where there is considerable restriction of the degrees of freedom of the reaction partners. The low ΔH^\ddagger values mean the catalytic reactions are particularly insensitive to temperature changes so that the phosphate cleavage reactions will proceed rapidly at low temperatures. The large ΔS^\ddagger terms dominate the free energy calculations, with the computed values for ΔG_{25}^\ddagger being about 4 and 3 kcal/mol lower than the ΔG_{25}^\ddagger for the corresponding methoxide reactions. Since there is no experimental difference between the ΔS^\ddagger terms for DMP and **4a**, one cannot say that the TS for the *o*- CO_2Me -bearing reactant is significantly more restricted than that for DMP.

g. Catalytic Rate Acceleration and Transition State Effects. The efficacy of catalyst-promoted reactions can be evaluated by comparing the free energy of binding of the catalyst to the TS of the presumed lyoxide-promoted reaction.^{43,44} The

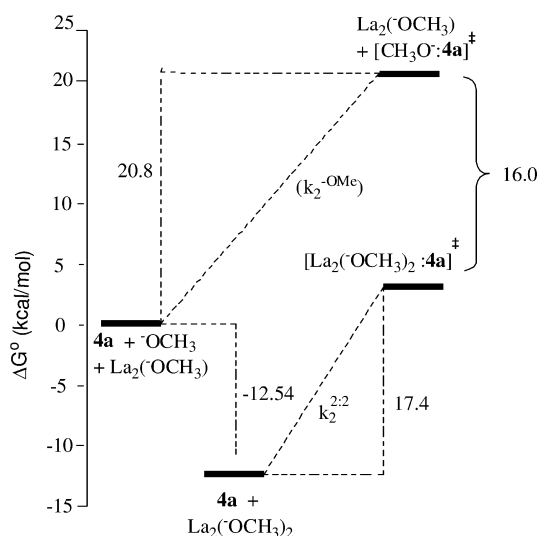


Figure 6. Activation energy diagram for the methoxide and the $[\text{La}_2(\text{OCH}_3)_2]$ -catalyzed cleavage of substrate **4a** at standard state 1 M and 25 °C, showing the calculated energy of binding methoxide by $\text{La}_2(\text{OCH}_3)_2$ and the activation energies associated with $k_2^{2:2}$ and $k_2^{-\text{OMe}}$. Free energies of activation are calculated as $\Delta G^\ddagger = -RT \ln(k_2/(kT/h))$ from the Eyring equation, where $(kT/h) = 6 \times 10^{12} \text{ s}^{-1}$ at 298 K.

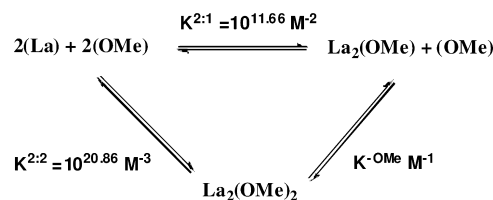


Figure 7. Thermodynamic cycle depicting the formation of $[\text{La}_2(\text{OMe})_2]$ and $[\text{La}_2(\text{OMe})_2]$ from free 2La^{3+} and $2(\text{OMe})$. The stability constants $K^{2:2}$ and $K^{2:1}$ were determined by fits of potentiometric data using the Hyperquad program as described.²⁵ Charges and associated counterions are omitted for clarity.

free energy diagram shown in Figure 6 shows the ΔG^\ddagger of activation for the methoxide reaction of **4a** and that of its $\text{La}_2(\text{OCH}_3)_2$ -catalyzed cleavage at the standard state of 1 M, $T = 25$ °C. In eq 5

$$\Delta\Delta G_{\text{stab}}^\ddagger = (\Delta G_{\text{bind}}^\ddagger + \Delta G_{\text{cat}}^\ddagger) - \Delta G_{-\text{OR}}^\ddagger = -RT \ln \left[\frac{(k_2^{2:2})(K^{-\text{OR}})}{k_2^{-\text{OMe}}} \right] \quad (5)$$

is the expression for determining the free energy of binding of the catalyst to the methoxide plus substrate in the TS, $\Delta\Delta G_{\text{stab}}^\ddagger$. The $\Delta G_{-\text{OR}}^\ddagger$ for the methoxide reaction was calculated to be 20.8 kcal/mol from the Eyring equation (eq 6) using $k_2^{-\text{OMe}} = 3.20 \times 10^{-3} \text{ M}^{-1} \text{ s}^{-1}$ (Table 1).

$$\Delta G_{-\text{OR}}^\ddagger = -RT \ln(k_2^{-\text{OR}}/(kT/h)) \quad (6)$$

The $K^{-\text{OR}}$ binding constant of $^-\text{OCH}_3$ to the catalyst (here taken to be $\text{La}_2(\text{OCH}_3)_2$) is calculated in accordance with the thermodynamic cycle in Figure 7, giving $K^{-\text{OMe}} = 10^{20.86}/10^{11.66} = 10^{9.2} \text{ M}^{-1}$, from which the free energy of binding is determined to be $\Delta G_{\text{bind}}^\ddagger = -RT \ln(K^{-\text{OMe}}) = -12.5$ kcal/mol.

(44) For applications of this to phosphate cleavage and other reactions, see: Yatsimirsky, A. K. *Coord. Chem. Rev.* **2005**, 249, 1997, and references therein.

(39) Liu, C. T.; Brown, R. S. Unpublished results.

(40) Ginjaar, L.; Vel, S. *Recl. Trav. Chim.* **1958**, 77, 956.

(41) The reported activation parameters for the hydroxide-promoted reaction of paraoxon are $\Delta H^\ddagger = 12.69 \pm 0.03$ kcal/mol and $\Delta S^\ddagger = -24.81 \pm 0.05$ cal/mol·K ($\Delta G_{25}^\ddagger = 20 \pm 0.3$ kcal/mol): Purcell, J.; Hengge, A. C. *J. Org. Chem.* **2005**, 70, 8437.

(42) Iché-Tarrat, N.; Barthelat, J.-C.; Rinaldi, D.; Vigroux, A. *J. Phys. Chem. B* **2005**, 109, 22570.

(43) Wolfenden, R. *Nature* **1969**, 223, 704.

Table 5. Computed Free Energies of Activation for the [La₂(OCH₃)_x]-Catalyzed Decomposition of **4a** (ΔG_{La}^\ddagger), Free Energy of Binding Methoxide to the Catalyst Precursor [La₂(OCH₃)_{x-1}] (ΔG_{bind}), Free Energy of Stabilization Afforded the Methoxide TS by Binding to the Active Catalyst [La₂(OCH₃)_x] ($\Delta\Delta G_{stab}^\ddagger$), and ${}^s pK_a^{Nuc}$ for the Formal La₂(OCH₃)_{x-1}(HOCH₃) ↔ La₂(OCH₃)_x + H₂O + CH₃ Ionization Process^a

	ΔG_{bind} (kcal/mol)	ΔG_{La}^\ddagger (kcal/mol)	$\Delta\Delta G_{stab}^\ddagger$ (kcal/mol)	${}^s pK_a^{Nuc}$
[La ₂ (OCH ₃) ₂]	12.54	17.35	15.99	7.56
[La ₂ (OCH ₃) ₃]	9.08	16.37	13.51	10.11
[La ₂ (OCH ₃) ₄]	9.59	17.36	13.03	9.73
[La ₂ (OCH ₃) ₅]	6.49	17.58	9.71	12.00

^a Stability constants and ${}^s pK_a^{Nuc}$ data for the various La₂(OCH₃)_x complexes are found in ref 25.

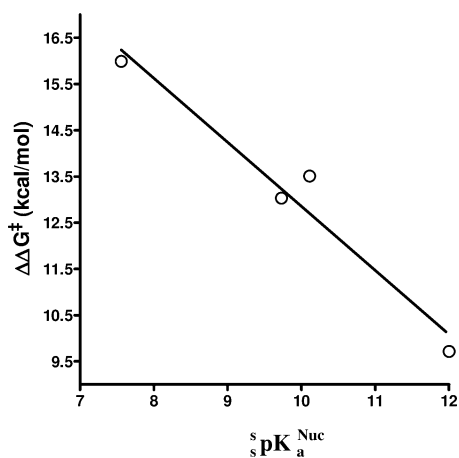


Figure 8. Plot of $\Delta\Delta G_{stab}^\ddagger$ versus ${}^s pK_a^{Nuc}$ of a molecule of methanol coordinated to the catalyst which fits a standard linear regression of $\Delta\Delta G_{stab}^\ddagger = (-1.39 \pm 0.21){}^s pK_a^{Nuc} + (26.7 \pm 2.1)$ kcal/mol, $r^2 = 0.9554$, four data.

The free energy of activation for La³⁺-catalyzed cleavage of **4a** is $\Delta G_{cat}^\ddagger = 17.4$ kcal/mol using the Eyring equation and the second-order rate constant $k_2^{2:2} = 1.11 \pm 0.21$ M⁻¹ s⁻¹ (Table 1). It can be seen from Figure 6 that the binding of La³⁺₂(⁻OCH₃) to the TS comprising **4a**⋯⁻OCH₃ is $\Delta\Delta G_{stab}^\ddagger = 16$ kcal/mol, which exceeds the stabilization afforded by binding methoxide in the ground state by ~3 kcal/mol.

Using the above procedure ΔG_{bind} , ΔG_{cat}^\ddagger , and $\Delta\Delta G_{stab}^\ddagger$ were calculated for each of the catalytic [La₂(OCH₃)_x] complexes, where $x = 2-5$, Table 5. It is notable that the Brønsted plot of the $k_2^{2:2}$ constants in Table 1 gives $\beta_{nuc} = -0.02 \pm 0.15$, indicating that the anticipated increase in rate constant with nucleophile ${}^s pK_a$ is not evident for this reaction. This is probably due to a counterbalancing electrophilic activation of the substrate coupled to the nucleophilic delivery of a La³⁺₂-bound methoxide.

The plot shown in Figure 8 of $\Delta\Delta G_{stab}^\ddagger$ vs ${}^s pK_a^{Nuc}$ for the last methoxide associated with the La³⁺₂(⁻OCH₃)_{x-1} catalyst fits a regression of $\Delta\Delta G_{stab}^\ddagger = (-1.39 \pm 0.21){}^s pK_a^{Nuc} + (26.7 \pm 2.1)$ kcal/mol, indicating that the catalytic proficiency of the system, relative to the methoxide reaction, increases by some 1.39 kcal/mol per unit decrease in ${}^s pK_a^{Nuc}$. The data in Table 5 show that the ΔG_{bind} values increase regularly with ${}^s pK_a^{Nuc}$ as expected, but there is only a small variation in the ΔG_{La}^\ddagger . Taken together, these suggest that the changes in ΔG_{bind} of methoxide for a given La³⁺₂(⁻OCH₃)_x complex are exactly compensated by changes to the $\Delta\Delta G$ for binding of the entire TS by that complex, so the ($\Delta\Delta G_{stab}^\ddagger - \Delta G_{bind}$) is essentially constant at ~3.4 kcal/mol. Put another way, whatever reduction in attractive energy occurs in loosening the association of the attacking methoxide and its

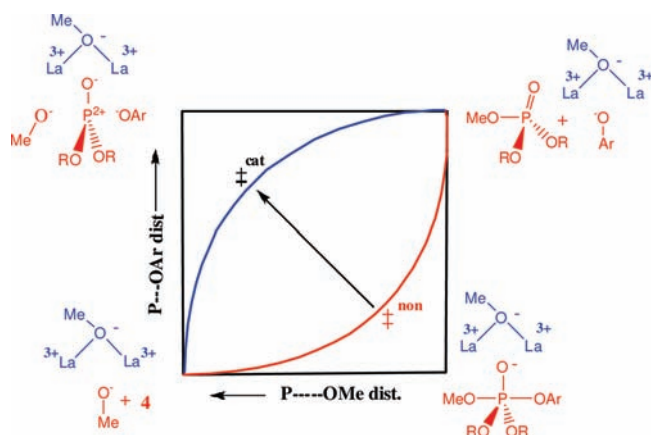


Figure 9. A reaction coordinate diagram for the cleavage of phosphate esters **4** depicting the trajectory taken by the reacting substrate through the potential energy surface in the presence (blue line) and absence (red line) of the La³⁺₂(⁻OMe) catalyst.

La³⁺₂(⁻OCH₃)_x parent in the TS is offset by a concomitant decrease in the attractive energy between the transforming substrate and La³⁺₂(⁻OCH₃)_{x-1}.

h. More O’Ferrall–Jencks Diagram⁴⁵ for the Catalyzed and Uncatalyzed Reactions. In accordance with linear free energy^{15,33,46} and computational^{42,47} data that indicate that oxyanion nucleophiles react via concerted processes with acyclic triesters having aryloxy leaving groups, we favor a concerted reaction for the reaction of methoxide with phosphate esters **3** and **4** in methanol. The noncatalyzed TS position (\ddagger^{non}) for this reaction with **4** (and **3**) is biased toward the phosphorane corner of Figure 9, in agreement with the small Leffler parameter ($\alpha = 0.27-0.32$) and the general consensus that neutral triesters react by tighter, associative TSs with the phosphoryl center accepting negative charge.¹⁵ In the diagram, the catalyst (formally La³⁺₂(OCH₃)₁ in blue) is positioned suggestively above the methoxide and phosphate reaction components (in red) at each of the four corners to illustrate the proposed binding of the catalyst. Both starting material and product are neutral phosphate triesters and thus are not bound, to any great extent, by any of the La³⁺₂ species. Methoxide is bound to La³⁺₂(OCH₃)₁ with $\Delta G_{bind} = 12.5$ kcal/mol, but this is expected to be partially counterbalanced by La³⁺₂(OCH₃)₁ binding to the aryl oxide in the product state. An exact ΔG_{bind} for the latter is not available but should be intermediate between an upper limit of 13.4 kcal/mol, as computed from the K_b for **4a** by spectrophotometric titration, and a lower limit of 10.5 kcal/mol, arrived at by extrapolation of the linear regression (Figure 5) for regular phenols to a ${}^s pK_a$ of 14.2, corresponding to a substrate of identical ${}^s pK_a$ to that of **4a** but lacking the *o*-CO₂Me substituent. These considerations indicate that the catalyst should have a minimal effect on the TS position along the reaction coordinate in the classic Hammond sense.

However, the fact that the β_{lg} values for the La³⁺-catalyzed cleavages of esters **3** and **4** are larger and more negative than the respective methoxide reactions indicates that the catalyzed TS (\ddagger^{cat}) has moved in the anti-Hammond sense toward the upper left corner, with considerable development of negative

(45) (a) More O’Ferrall, R. A. *J. Chem. Soc. B* **1970**, 274. (b) Jencks, W. P. *Chem. Rev.* **1972**, 72, 705.

(46) Lewis, V. E.; Donarski, W. J.; Wild, J. R.; Rauschel, F. M. *Biochemistry* **1988**, 27, 1591.

(47) Zheng, F.; Zhan, C.-G.; Ornstein, R. L. *J. Chem. Soc., Perkin Trans. 2* **2001**, 2355.

charge on the leaving group, implying a far looser TS. Additionally, the β_{nuc} of -0.02 ± 0.15 for the data in Table 1 and the TS stabilization ($\Delta\Delta G_{\text{stab}}^{\ddagger}$ in Figure 6) of 16 kcal/mol, which exceeds the ΔG_{bind} of methoxide to $\text{La}_2(\text{OMe})_1$ by over 3 kcal/mol, demonstrate that the role of the catalyst in promoting the cleavage of phosphate esters **4** is to bind *all* the components of the loose TS, with delivery of a La^{3+} -bound methoxide to a phosphoryl group that is electrophilically activated by metal ion coordination. In the catalyzed reactions of **3**, not containing the *o*- CO_2Me group, the departing aryl oxide can be stabilized electrostatically by the positively charged catalytic system. However, esters **4**, with the *o*- CO_2Me group, exhibit an additional coordinative interaction with the metal ions that provides modest but real electrophilic assistance to the leaving group departure.

5. Conclusions

The common feature between dinuclear Zn(II)-containing PTEs and the La^{3+} -catalyzed cleavage of phosphate triesters is the large negative Brønsted β_{lg} , indicating substantial cleavage of the P–OAr bond in the TS. A consequence of this is evident from inspection of Figure 3, where a convergence of the La^{3+} - and methoxide-catalyzed Brønsted plots at high $\text{p}K_{\text{a}}$ indicates that substrates with good leaving groups are accelerated disproportionately by the catalyst relative to substrates with poor leaving groups, ($|\beta_{\text{lg}}^{\text{cat}}| > |\beta_{\text{lg}}^{\text{OR}^-}|$). Leaving group assistance would be optimized and generally desirable in situations where a catalyst (enzyme) needs to select for substrates with poor leaving groups relative to those with good leaving groups ($|\beta_{\text{lg}}^{\text{cat}}| < |\beta_{\text{lg}}^{\text{OR}^-}|$). Since the neutral OP phosphate esters that are toxic to organisms are those having leaving groups of $\text{p}K_{\text{a}} \leq 8$, there is no evolutionary pressure for the PTEs to build in LGA to the catalytic machinery for cleaving these types of OP materials.

To probe whether LGA is possible for our synthetic PTE system comprising La^{3+} -catalysis of phosphate triesters in alcohol, we have employed a series of phosphate triesters having aryloxy leaving groups with an *o*- CO_2Me which were previously shown to induce LGA to the metal-catalyzed cleavage of phosphate diesters.²² Here, the three-fold demonstration of (1) a less negative β_{lg} for the Brønsted plot of the catalyzed reaction,

(2) a faster rate of cleavage for *o*- CO_2Me -containing substrates relative to ones with the same leaving group $\text{p}K_{\text{a}}$ but not having the *o*- CO_2Me group, and (3) cleavage products that are metal-complex-bound phenoxides indicates that these specially designed neutral OP triester substrates are subject to modest but real LGA. Our preferred mechanism for this process is a concerted one where the catalyst binds to all three components of a rather exploded TS, namely the nucleophilic $^-\text{OCH}_3$, ^-OAr nucleofuge, and a central $(\text{RO})_2\text{P}^{2+}-\text{O}^-$ unit bridged between a catalytic $\text{La}^{3+}_2(\text{OCH}_3)_{x-1}$ entity. Enzymatic mechanisms for phosphoryl transfer involving LGA through transition states resembling that offered here in Scheme 2 have been proposed for dinuclear M(II) phosphodiesterases,⁴⁸ for alkaline phosphatase,⁴⁹ and in an early paper^{16b} for PTE, although there is no general consensus for the latter's mechanism of operation.⁵⁰

Acknowledgment. The authors gratefully acknowledge the financial assistance of the Natural Sciences and Engineering Research Council of Canada. This project received support (grant no. HDTRA1-08-1-0046) from the Defense Threat Reduction Agency–Joint Science and Technology Office, Basic and Supporting Sciences Division. C.T.L. thanks NSERC Canada for a PGS-D postgraduate scholarship (2006–2010).

Supporting Information Available: Tables of observed pseudo-first-order rate constants for the methoxide-promoted cleavage of substrates **3** and **4** and plots of k_{obs} vs $[\text{La}^{3+}]_{\text{total}}/2$; supporting text describing procedures for the synthesis of all compounds used in this study and their NMR data, attempted data treatment with Jaffé equation, and experimental procedure for the Job plot of **4c**. This material is available free of charge via the Internet at <http://pubs.acs.org>.

JA904659E

(48) Steitz, T. S.; Steitz, J. A. *Proc. Natl. Acad. Sci. U.S.A.* **1993**, *90*, 6498.

(49) (a) Kim, E. E.; Wyckoff, H. W. *J. Mol. Biol.* **1991**, *218*, 449. (b) Holtz, K. M.; Stec, B.; Kantrowitz, E. R. *J. Biol. Chem.* **1999**, *274*, 8351. (c) Zalatan, J. G.; Herschlag, D. *J. Am. Chem. Soc.* **2006**, *128*, 1293.

(50) (a) Wong, K.-Y.; Gao, J. *Biochemistry* **2007**, *46*, 13352. (b) Samples, C. R.; Raushel, F. M.; DeRose, V. J. *Biochemistry* **2007**, *46*, 3435. (c) Liu, J.-W.; Salem, G.; Ollis, D. L. *J. Mol. Biol.* **2008**, *375*, 1189.